Sliding mode control with neural network for active magnetic bearing system

Cao, Zhi; Dong, Jianning; Wani, Faisal; Polinder, Henk; Bauer, Pavol; Peng, Fei; Huang, Yunkai

DOI
10.1109/IECON.2019.8926808

Publication date
2019

Document Version
Final published version

Published in
Proceedings

Sliding Mode Control with Neural Network for Active Magnetic Bearing System

Zhi Cao[†*], Jianning Dong[*‡], Faisal Wani[*], Henk Polinder[*], Pavol Bauer[*], Fei Peng[†], Yunkai Huang[†]
[*]Faculty of EEMCS, Delft University of Technology, Delft, The Netherlands
[†]School of Electrical Engineering, Southeast University, Nanjing, China
[‡]J.Dong-4@tudelft.nl

***Abstract*—A novel controller design procedure is proposed for a 5-degree-of-freedom (DOF) active magnetic bearing (AMB) system, based on sliding mode control (SMC) and neural network (NN). The SMC is used to achieve high robustness and fast response while the NN can compensate unmodeled uncertainty and external disturbance by on-line tuning algorithm. The proposed controller is compared with the well-tuned PID controller by simulations. The simulation results show the superior performance of the proposed controller.**

***Index Terms*—magnetic bearing, neural network, sliding mode control.**

I. Introduction

The active magnetic bearings (AMB) allows operation with reduced friction and mechanical wearing. Compared with other types of non-contact bearings like hydrostatic/hydrodynamic bearings and air bearings, it is able to actively control the rotordynamics and requires less maintenance, which makes it appealing for applications including flywheels and turbine generators [1].

The AMB system is an inherently unstable system with strong nonlinearities, coupled dynamics and uncertainties. Various control strategies have been proposed to improve the AMB performance. Proportional-integral-derivative (PID) control is widely used for the AMB systems because of its simplicity [1]. However, PID control cannot may not provide acceptable performance since it largely ignores model uncertainty and coupled dynamics in the AMB system [2]. Robust control methods, including H_∞ and μ-synthesis, provide an efficient way to design robust controllers with the ability to handle parametric uncertainties and external disturbance for the AMB system [2] [3]. These controllers require accurate model, which is mathematically demanding and complex to identify. Besides, the order of controllers used in these methods is high. For example, a 10^{th} μ-controller was designed in [4]. Nonlinear control approaches such as feedback linearization, sliding mode control (SMC) and adaptive control are also used. Feedback linearization method is based on the nonlinear model of the AMB, which guarantees controller effectiveness in the whole operation range [5]. However, it is parametrically sensitive. In [6], a robust nonsingular terminal sliding mode controller for the AMB achieves fast, finite time convergence and good precision but it is based on a linearized electromagnetic force model. Adaptive control is used to suppress external disturbance in [7]. Moreover, combinations of different control methods and intelligent algorithms such as neural network and fuzzy logic control can enhance the control performance [6] [8].

This paper proposes a controller for AMB which applies basic SMC and a one-layer neural network (NN) to compensate the unmodeled uncertainties of the system. The controller is analyzed and verified through simulations. The proposed controller is compared with the conventional PID controller. Compared to previous work, the proposed controller achieves good trade-off between complexity and effectiveness.

The work was supported by the China Scholarship Council (CSC) and the TiPA project (Tidal turbine Power take-off Accelerator), which has received funding from the European Union's Horizon 2020 research and innovation programme under grant agreement No. 727793, managed by the Innovation and Networks Executive Agency. This paper reflects only the authors' view, the Agency is not responsible for any use that may be made of the information the paper contains.

II. System Model

The paper investigates a 5-degree-of-freedom (DOF) AMB prototype for a direct-drive permanent magnet wind turbine concept, as is shown in Fig. 1. Design and parameters of the prototype are presented in [9], [10]. Four pairs of axial actuators and two pairs of radial actuators are used in this setup. The actuators are U-core electromagnets.

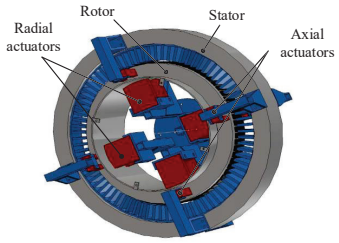

Fig. 1: A 5-DOF AMB setup integrated into a permanent magnet wind turbine [10].

In this paper, decentralized control strategy is adopted. Each pair of actuator is controlled independently for simplicity. Assume the rotor is rigid, the dynamic model of 1-DOF AMB-rotor system can be described as

$$m\ddot{x} = F_a + F_d = f(i, x) + F_d \tag{1}$$

where x is the displacement of the rotor in either direction, i the actuator current, m the mass of the rotor, F_d the external

978-1-7281-4878-6/19/$31.00 ©2019 IEEE

disturbance, F_a the magnetic force generated by a pair of actuators. The magnetic force is related to the displacement and current and can be given approximately by [1]:

$$F_a \approx \hat{f}(i,x) = \frac{\mu_0 S N^2}{4}\left(\frac{i}{g_0 \pm x}\right)^2 = k\left(\frac{i}{g_0 \pm x}\right)^2 \quad (2)$$

where μ_0 is the magnetic permeability in the air, S the sectional area of the actuator, N the number of coil, g_0 the nominal air gap length.

III. Proposed Controller

A cascaded controller design procedure for the 1-DOF AMB system is proposed as follows:

1) Design the position controller to keep the rotor at the desired position and obtain the desired force;
2) Deduce the desired current according to the relationship between the force and current;
3) Design the current controller which can follow the current command obtained in the last step and generate the final voltage input.

The proposed design procedure based on a nonlinear electromagnetic force model (2). In step 2), the desired current can be deduced by (2)

$$\hat{i} = \hat{f}^{-1}(F_a, x) \quad (3)$$

However, it cannot precisely describe the relationship of the force versus current and displacement as it does not account for nonlinearities like saturation. As a result, it would introduce unmodeled error

$$\Delta = f\left(\hat{f}^{-1}\left(F_a,x\right),x\right) - \hat{f}\left(\hat{f}^{-1}\left(F_a,x\right),x\right) \quad (4)$$

The dynamics of the 1-DOF system can be rewritten as

$$m\ddot{x} = F_a + F_d + \Delta \quad (5)$$

A. Position Controller Design

Considering nonlinearity and uncertainty of the AMB system and demand of the controller in accuracy and robustness, SMC with NN controller is proposed. Sliding mode control is the main control and neural network is used to compensate the unmodeled uncertainty and external disturbance in (5).

Firstly, define the sliding variable with the position error as

$$s = ce + \dot{e} \quad (6)$$

where $e = x_d - x$, x_d is the desired displacement, c is a positive constant.

The derivative of the sliding variable can be deduced as

$$\dot{s} = c\dot{e} + \ddot{x}_d - m^{-1}\left(F_a + F_d + \Delta\right) \quad (7)$$

Reaching law method is applied here to obtain a switching control input and ensure stability and dynamic response [11]. The reaching law is given by

$$\dot{s} = -k_s s - \delta sgn\left(s\right) \quad (8)$$

where $sgn(s)$ is a sign function, k_s and δ are the gains.

According to equation (7) and (8), we can design the control input as

$$u = u_{smc} - u_{nn} \quad (9)$$

where

$$u_{smc} = m\left(c\dot{e} + \ddot{x}_d + k_s s + \delta sgn(s)\right) \quad (10)$$

u_{nn} is the neural network term to compensate the unmodeled structure Δ and external disturbance F_d.

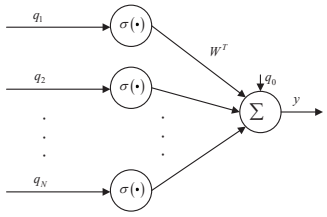

Fig. 2: One-layer neural network, where q_i are inputs and y is output.

According to [12], one-layer functional-link neural network (FLNN), of which the structure is shown in Fig. 2, can serve as the function approximator. Then, the unmodeled structure error and external disturbance can be approximated as

$$\Delta + F_d = W^T\sigma(q) + \epsilon \quad (11)$$

with the estimation error bounded by $\|\epsilon\| < \epsilon_N$.

The input of the NN is selected as $q = \begin{bmatrix} e & \dot{e} \end{bmatrix}^T$ and it is bounded by

$$\|q\| \le c_1 + c_2|s| \quad (12)$$

for computable positive constants c_i (c_2 decreases as c increases) [12].

W is the ideal approximating weights, which are unknown and may even be nonunique. Assume the ideal weights are constant and bounded by

$$\|W\|_F \le W_B \quad (13)$$

with the bound W_B known. The $\|*\|_F$ denotes the Frobenius norm.

$\sigma(q)$ is the activation function and here we select sigmoid function

$$\sigma(q) = \frac{1}{1+e^{aq}} \quad (14)$$

Then, an estimate of (11) is given by

$$u_{nn} = \hat{W}^T\sigma\left(q\right) \quad (15)$$

where $\hat{W}$ is the current actual weights as provided by the tuning law to be specified.

Substituting (10) and (15) into (7) yeilds

$$\dot{s} = -k_s s - \delta sgn(s) - m^{-1}\left(\tilde{W}^T\sigma\left(q\right) + \epsilon\right) \quad (16)$$

where $\tilde{W} = W - \hat{W}$.

Given the tuning laws

$$\dot{\hat{W}} = m^{-1}\left(-F\sigma s - \kappa F\left|s\right|\hat{W}\right) \quad (17)$$

with any constant matrices $F = F^T > 0$ and small scalar parameters $\kappa > 0$. Then for large enough k_s, the sliding surface s and the NN weight estimates $\hat{W}$are ultimately uniformly bounded (UUB). Moreover, the tracking error can be made smaller by increasing the gain k_s.

Proof: Let the NN approximation property (11) hold for the function $\Delta + F_d$ with a given accuracy ϵ_N for all q in the compact set $S_q = \{q| \|q\| < b_q\}$. Define $S_s = \{s| \|r\| < (b_q - c_1)/c_2\}$. Let $s(0) \in S_x$. Then the approximation holds.

Select the Lyapunov function candidate as

$$L = \frac{1}{2}s^2 + \frac{1}{2}tr\left(\tilde{W}^T F^{-1}\tilde{W}\right) \tag{18}$$

Differentiating it yields

$$\dot{L} = s\dot{s} + tr\left(\tilde{W}^T F^{-1}\dot{\tilde{W}}\right) \tag{19}$$

Since $\dot{\tilde{W}} = -\dot{\hat{W}}$, substituting tuning rules (17) and reaching law (8) into (19) yields

$$\begin{aligned}\dot{L} = &- k_s s^2 - \delta|s| \\ &+ m^{-1}\kappa|s| tr\tilde{W}^T\left(W - \tilde{W}\right) - m^{-1}s\epsilon\end{aligned} \tag{20}$$

Since

$$\begin{aligned}tr\tilde{W}^T\left(W - \tilde{W}\right) &= \left\langle \tilde{W}, W\right\rangle_F - \left\|\tilde{W}\right\|_F^2 \\ &\le \left\|\tilde{W}\right\|_F \|W\|_F - \left\|\tilde{W}\right\|_F^2\end{aligned} \tag{21}$$

Then

$$\begin{aligned}\dot{L} \le &- k_s|s|^2 - \delta|s| \\ &+ m^{-1}\kappa|s|\left\|\tilde{W}\right\|_F\left(W_B - \left\|\tilde{W}\right\|_F\right) - m^{-1}\epsilon_N|s| \\ &= -|s| \\ &\times\left[k_s|s| + \delta + m^{-1}\kappa\left\|\tilde{W}\right\|_F\left(\left\|\tilde{W}\right\|_F - W_B\right) + m^{-1}\epsilon_N\right]\end{aligned} \tag{22}$$

which is negative as long as the term in square braces is positive. Completing the square yields

$$\begin{aligned}&k_s|s| + \delta + m^{-1}\kappa\left\|\tilde{W}\right\|_F\left(\left\|\tilde{W}\right\|_F - W_B\right) + m^{-1}\epsilon_N \\ &= m^{-1}\kappa\left(\left\|\tilde{W}\right\|_F - W_B/2\right)^2 \\ &- m^{-1}\kappa {W_B}^2/4 + k_s|s| + \delta + m^{-1}\epsilon_N\end{aligned} \tag{23}$$

which is positive as long as

$$|s| > \frac{\kappa {W_B}^2/4 - \epsilon_N - m\delta}{mk_s} = b_s \tag{24}$$

or

$$\left\|\tilde{W}\right\|_F > W_B \tag{25}$$

Thus, $\dot{L}$ is negative outside a compact set. A large enough gain k_s can ensure the compact set (24) contained in S_s, i.e.,

$$k_s > \frac{c_2\left(\kappa {W_B}^2/4 - \varepsilon_N - m\delta\right)}{m\left(b_q - c_1\right)} \tag{26}$$

so that the approximation property holds throughout. This demonstrates the UUB of $|s|$ and $\left\|\tilde{W}_F\right\|$. ■

The NN weights can be initialized at zero, and stability will be provided by the sliding mode control term until NN learns, which means there is no need for off-line learning and learning process occurs in real-time.

B. Deduction of Desired Current

Once the desired force is obtained, the desired current commands of a pair of actuators can be given by

$$\begin{aligned}if \quad F_a > 0 &\begin{cases} i_1 = \sqrt{F_a/k}(g_0 - x) \\ i_2 = 0 \end{cases} \\ if \quad F_a < 0 &\begin{cases} i_1 = 0 \\ i_2 = \sqrt{F_a/k}(g_0 - x) \end{cases}\end{aligned} \tag{27}$$

where i_1 and i_2 are the currents of two coils in a pair of actuators.

This zero-bias current control scheme can reduce the power loss compared with biased current control. Furthermore, the PI controller is applied in this paper for the current regulation. Also, more advanced current controllers can be designed with other methods but it is out of scope of this paper.

The proposed controller is designed in continuous domain and it is discretized by Euler's Method when applied with digital control system. In addition, as can be seen from the design process above, the velocity information is needed. Therefore, phase-lock-loop (PLL) is designed to calculate the rotor position and velocity as follows [13]

$$\begin{aligned}\hat{x}(n+1) &= \hat{x}(n) + \hat{v}(n)T_s + K_n T_s e(n) \\ \hat{v}(n+1) &= \hat{v}(n) + K_v T_s e(n)\end{aligned} \tag{28}$$

where $\hat{x}(n)$ is the estimated displacement for the current sampling step, $\hat{x}(n+1)$ is the estimated displacement for the next sampling step, $\hat{v}(n)$ is the estimated speed for the current sampling step, $\hat{v}(n+1)$ is the estimated speed for the next sampling step, the current estimated error is $e(n) = x(n) - \hat{x}(n)$, T_s is the sample time, K_n and K_v are the coefficients of PLL.

The overview schematic diagram of the proposed controller for the 5-DOF AMB system is presented in Fig. 3. Each pair of actuator is controlled by a independent local controller to keep the rotor at the desired position, and all the local controllers have the same structures as designed above.

IV. Simulation Results

A. Parameter Setting of Simulation Model

The parameters of AMB-rotor system are presented in Table I. To simulate the actuators properly, a finite element (FE)-based look-up table (LUT) model of the actuator is developed in this paper. FE analysis can generate flux LUTs $\psi(i,x)$ and force LUTs $f(i,x)$. The flux LUTs $\psi(i,x)$ are inverted to the LUTs $i(\psi,x)$ to avoid simulation errors caused by numerical differential operation and make it convenient to use the voltage as the input when considering the voltage source inverter.

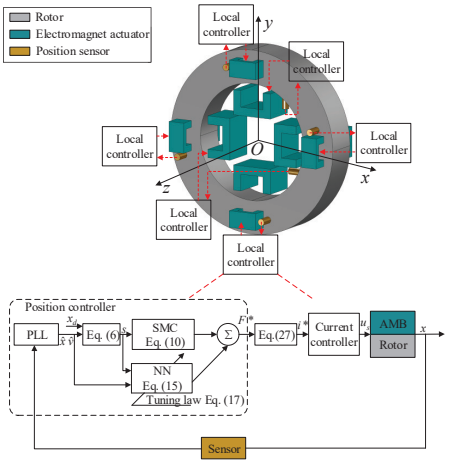

Fig. 3: Overview of the controller structure for a 5-DOF AMB-rotor system.

TABLE I: Parameters of the AMB-rotor system

Parameter	Value
Mass of rotor	5 kg
Nominal air gap length	1.5 mm
Number of turns (radial actuator)	430
Sectional area (radial actuator)	700 mm^2
Resistance of coil (radial actuator)	2.25 Ω
Number of turns (axial actuator)	200
Sectional area (axial actuator)	240 mm^2
Resistance of coil (axial actuator)	0.6 Ω
DC voltage supply	50 V

Therefore, a FE-based LUT dynamic model is proposed as shown in Fig. 4, where R_c is the resistance of the coil.

In this work, the performance of the proposed controller is compared with well-tuned PID controller which is designed based on the linearized model in [1] to demonstrate the effectiveness and the superiority of the proposed method. The final designed control parameters are given in Table II. The simulations are implemented in MATLAB/Simulink environment with 10 kHz sample frequency.

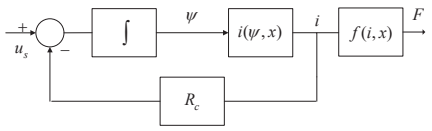

Fig. 4: Schematic of FE-based LUT model of an actuator.

TABLE II: Design values of the controller coefficients

Control scheme	design values
PID	$K_p = 4000$, $K_i = 60000$, $K_d = 13$
SMC with NN	$c = 100$, $k_s = 800$, $\delta = 0.1$, $F = diag[25 \quad 25]$, $\kappa = 0.0004$

B. One-DOF AMB System Simulation Results

The first case is the 1-DOF AMB-rotor system. The comparative simulation results of the displacement response of the proposed controller against PID controller are shown in Fig. 5. The rotor starts up at the half of the clearance at one side, and at the time 1s, a 100N step disturbance is loaded to the rotor, then at the time 2s unloaded. One can notice that both controllers can keep the rotor at the center while the proposed controller has better dynamics than PID controller, i.e., the proposed controller has smaller overshoot and shorter settling time than PID controller, especially during start-up. Fig. 6 are the control current results of two controllers and the copper losses of the coils. The copper loss of the proposed controller is less than a quarter of that of PID controller when only with dead weight. As is shown in Fig. 7, the one-layer NN can effectively and precisely compensate the unmodeled error and external disturbance in real-time. Additionally, to verify the robustness of the controllers, random noises are introduced to the sensors, and the displacement results are given in Fig. 8. It is apparent that the effect of noises is better suppressed by the proposed controller and the displacement fluctuation is smaller.

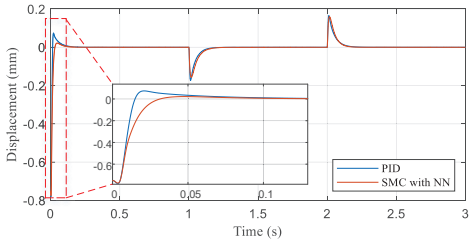

Fig. 5: Comparative simulation results of the displacement response of the proposed controller against PID controller for the 1-DOF system.

C. Five-DOF AMB System Simulation Results

The detailed simulation model of the 5-DOF AMB-rotor system is given in the Appendix. The displacement responses in X, Y, Z direction of the proposed controller and PID controller are shown in Fig. 9. The rotor rotation speed is 0 RPM ,and it starts up at the position of $(g_0/2, g0/3, -g0/2)$. At the time 1s, a 50N step disturbance is loaded to the rotor in Z direction, then at the time 2s unloaded. Besides, measurement noises are added in the path of sensors. The overshoot is lower and the response is faster with the proposed controller. In the meantime, it has the ability to suppress the effect of noises. Fig. 10 shows the trajectory of the rotor center.

Furthermore, the performance of two controllers are compared to investigate the gyroscopic effect on the system when the rotor rotation speed is nonzero. Fig. 11 gives the rotational angles around X-axis and Y-axis α, β when the rotor speed is 600 RPM and the disturbance condition is the same as above. One can notice that the proposed controller has better performance on compensate the gyroscopic effect. From these

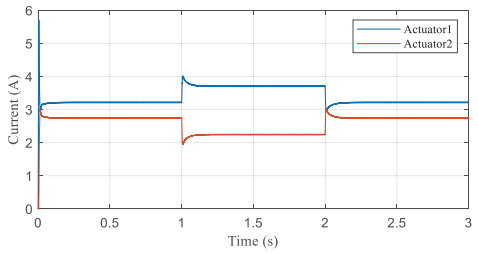

(a)

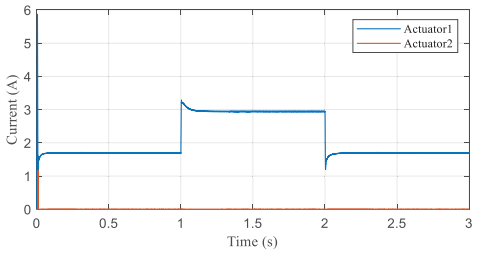

(b)

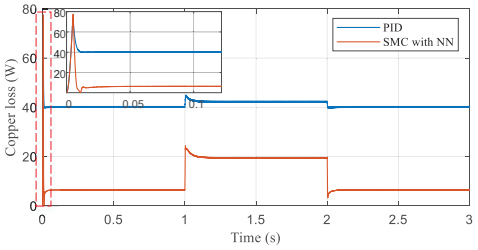

(c)

Fig. 6: Comparative simulation results of the control currents and copper losses: (a) PID controller; (b) proposed controller; (c) copper losses comparison.

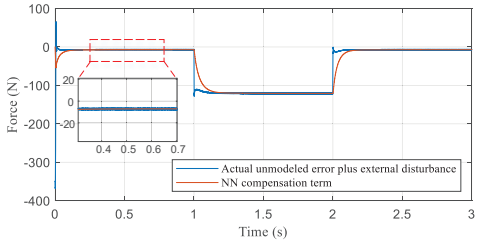

Fig. 7: Comparison between the compensation term obtained by neural network with actual unmodeled error plus external disturbance.

results, it can be concluded that the proposed controller can achieve better dynamics and robustness.

V. Conclusions

In this paper, a novel controller design procedure is presented to achieve dynamic response, stability and robustness as well as low loss for the AMB system. The dynamic model of the system is first established. To handle the high nonlinearity and uncertainty in the system, the SMC with NN controller is designed to control the rotor position, and zero-biased current

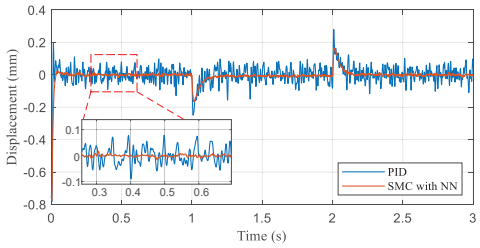

Fig. 8: Displacement response of the proposed controller and PID controller with measurement noise in the sensor for the 1-DOF system.

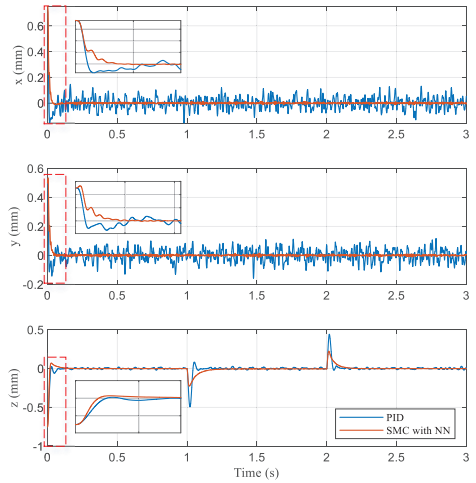

Fig. 9: Displacement response in X, Y, Z direction of the proposed controller and PID controller with measurement noise for the 5-DOF system (Rotor speed is 0 RPM).

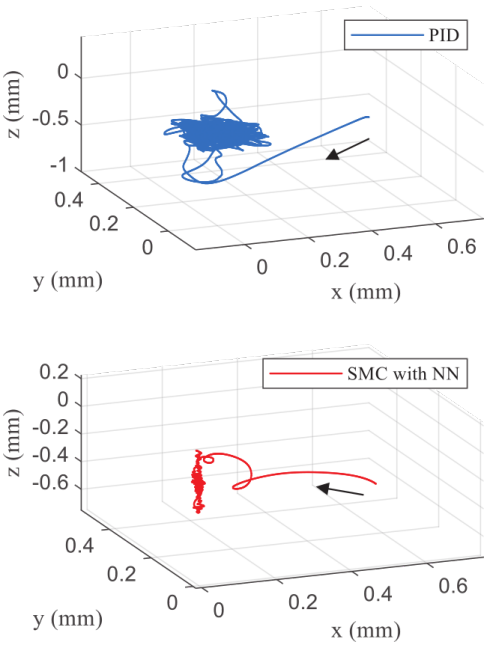

Fig. 10: Trajectory of the rotor center with the proposed controller and PID controller for the 5-DOF system (rotor speed is 0 RPM).

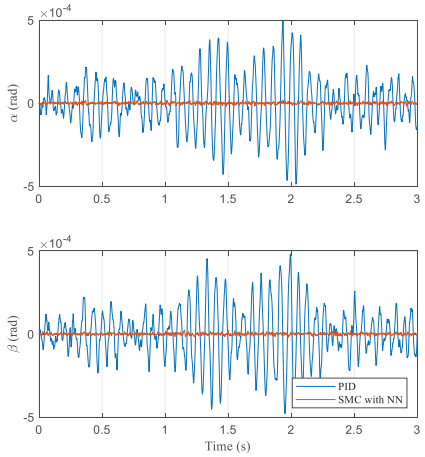

Fig. 11: Rotation motions with respect to X-axis and Y-axis of the 5-DOF system rotor with the proposed controller and PID controller (Rotor speed is 600 RPM).

control strategy is adopted here to reduce the copper loss. Simulations are performed to compare the performance of the proposed controller and the well-tuned PID controller. The simulation results show high precision, fast dynamic response and the ability to compensate the uncertain factors of the proposed controller. Besides, using one-layer NN with two neurons decreases the computation complexity as much as possible. Discussion on the trade-off between complexity and effectiveness would be included in future work, though.

APPENDIX

Assume that the rotor is symmetric and rigid; sensors and the corresponding actuators are in the same position, the 5-DOF AMB-rotor dynamic is given in the center of gravity (COG) coordinate system as

$$\mathbf{M}\ddot{\mathbf{q}}_\mathbf{c} + \mathbf{G}\dot{\mathbf{q}}_\mathbf{c} = \mathbf{B}\mathbf{F} + \mathbf{F}_\mathbf{d}$$

where

$$\mathbf{q_c} = \begin{bmatrix} x & y & z & \alpha & \beta \end{bmatrix}^T$$

$$\mathbf{F} = \begin{bmatrix} F_1 & F_2 & F_3 & F_4 & F_5 & F_6 \end{bmatrix}^T$$

$$\mathbf{M} = \begin{bmatrix} m & 0 & 0 & 0 & 0 \\ 0 & m & 0 & 0 & 0 \\ 0 & 0 & m & 0 & 0 \\ 0 & 0 & 0 & I_{yy} & 0 \\ 0 & 0 & 0 & 0 & I_{xx} \end{bmatrix}$$

$$\mathbf{G} = \begin{bmatrix} 0 & 0 & 0 & 0 & 0 \\ 0 & 0 & 0 & 0 & 0 \\ 0 & 0 & 0 & 0 & 0 \\ 0 & 0 & 0 & 0 & -\omega I_{zz} \\ 0 & 0 & 0 & \omega I_{zz} & 0 \end{bmatrix}$$

$$\mathbf{B} = \begin{bmatrix} 1 & 0 & 0 & 0 & 0 & 0 \\ 0 & 1 & 0 & 0 & 0 & 0 \\ 0 & 0 & 1/4 & 1/4 & 1/4 & 1/4 \\ 0 & 0 & R_r & 0 & -R_r & 0 \\ 0 & 0 & 0 & R_r & 0 & -R_r \end{bmatrix}$$

and x, y, z are the translational displacements on the three dimensions and α, β are the rotational angles around X-axis and Y-axis. F_1 to F_6 are the magnetic forces generated by six pairs of actuators respectively. I_{xx}, I_{yy}, I_{zz} are the moments of inertia respect to X, Y and Z axis. ω is the rotor speed. R_r is the radius of the rotor. The matrix $\mathbf{G}$ is called gyroscopic effect matrix.

The outputs of the rotor system are the displacements obtained by six sensors, i.e.,

$$\mathbf{q_s} = \begin{bmatrix} x_s & y_s & z_{1s} & z_{2s} & z_{3s} & z_{4s} \end{bmatrix}^T$$

$$\mathbf{q_s} = \mathbf{C}\mathbf{q_c}$$

where

$$\mathbf{C} = \begin{bmatrix} 1 & 0 & 0 & 0 & 0 \\ 0 & 1 & 0 & 0 & 0 \\ 0 & 0 & 1 & R_r & 0 \\ 0 & 0 & 1 & 0 & -R_r \\ 0 & 0 & 1 & -R_r & 0 \\ 0 & 0 & 1 & 0 & R_r \end{bmatrix}$$

REFERENCES

[1] E. H. Maslen and G. Schweitzer, Eds., *Magnetic Bearings: Theory, Design, and Application to Rotating Machinery*. Springer, Berlin, Heidelberg, 2009.

[2] S. E. Mushi, Z. Lin, and P. E. Allaire, "Design, construction, and modeling of a flexible rotor active magnetic bearing test rig," *IEEE/ASME Trans. Mechatronics*, vol. 17, no. 6, pp. 1170–1182, Dec 2012.

[3] A. Noshadi, J. Shi, W. S. Lee, P. Shi, and A. Kalam, "System identification and robust control of multi-input multi-output active magnetic bearing systems," *IEEE Trans. Control Syst. Technol.*, vol. 24, no. 4, pp. 1227–1239, July 2016.

[4] J. Fang, S. Zheng, and B. Han, "AMB vibration control for structural resonance of double-gimbal control moment gyro with high-speed magnetically suspended rotor," *IEEE/ASME Trans. Mechatronics*, vol. 18, no. 1, pp. 32–43, Feb 2013.

[5] A. Mystkowski and E. Pawluszewicz, "Feedback linearization of extended relative degree model of nonlinear active magnetic bearing system," in *2016 21st International Conference on Methods and Models in Automation and Robotics (MMAR)*, Aug 2016, pp. 460–465.

[6] S. Chen and F. Lin, "Robust nonsingular terminal sliding-mode control for nonlinear magnetic bearing system," *IEEE Trans. Control Syst. Technol.*, vol. 19, no. 3, pp. 636–643, May 2011.

[7] L. Dong and S. You, "Adaptive control of an active magnetic bearing with external disturbance," *ISA Trans.*, vol. 53, no. 5, pp. 1410–1419, 2014.

[8] K.-Y. Chen, P.-C. Tung, M.-T. Tsai, and Y.-H. Fan, "A self-tuning fuzzy pid-type controller design for unbalance compensation in an active magnetic bearing," *Expert Syst. Appl.*, vol. 36, no. 4, pp. 8560–8570, 2009.

[9] G. Shrestha, "Structural flexibility of large direct drive generators for wind turbines," Ph.D. dissertation, Delft University of Technology, 2013.

[10] G. Shrestha, H. Polinder, D. Bang, and J. A. Ferreira, "Structural flexibility: A solution for weight reduction of large direct-drive wind-turbine generators," *IEEE Trans. Energy Convers.*, vol. 25, no. 3, pp. 732–740, Sep. 2010.

[11] W. Gao and J. C. Hung, "Variable structure control of nonlinear systems: a new approach," *IEEE Trans. Ind. Electron.*, vol. 40, no. 1, pp. 45–55, Feb 1993.

[12] F. Lewis, S. Jagannathan, and A. Yesildirak, *Neural network control of robot manipulators and non-linear systems*. CRC Press, 1998.

[13] F. Peng, J. Ye, A. Emadi, and Y. Huang, "Position sensorless control of switched reluctance motor drives based on numerical method," *IEEE Trans. Ind. Appl.*, vol. 53, no. 3, pp. 2159–2168, 2017.